JOURNAL OF GEOPHYSICAL RESEARCH, VOL. 103, NO. A3, PAGES 4657–4669, MARCH 1, 1998

Multisatellite and ground-based observations of a tailward propagating Pc5 magnetospheric waveguide mode

Ian R. Mann,[1] Gareth Chisham, and Stuart D. Bale [2]
Astronomy Unit, Queen Mary and Westfield College, London, United Kingdom

Abstract.
Using data from the Active Magnetospheric Particle Tracer Explorers (AMPTE) Charge Composition Explorer (CCE) satellite near local noon, and the AMPTE Ion Release Module (IRM) and United Kingdom Subsatellite (UKS) on the morning flank, we investigate the tailward propagation of a compressional Pc5 wave (380 s period) on October 28, 1984, and suggest that the observation represents a magnetospheric waveguide mode. The observed wave is a transient oscillation lasting about five wave cycles with an observed time of flight from CCE to IRM/UKS of 180 s. The first three or four cycles at the leading edge of the event display a remarkable wave packet coherence between CCE and IRM/UKS despite their large separation in the magnetosphere ($\sim 6.2\ R_E$). A time of flight analysis suggests a waveguide mode group speed ~ 220 km s^{-1}, being much less than the local Alfvén speed and comparable to the expected sub-Alfvénic propagation speed of a waveguide mode. The ground-based signature of the event is also observed near local noon by the European Incoherent Scatter magnetometer cross, displaying the same period and lasting for the same number of cycles. The ground-based data show no evidence of a field line resonance; the event is monochromatic, and there is little variation of amplitude and polarization with latitude. An increase in solar wind ram pressure of $\sim 30\%$ is observed by IMP 8 upstream in the solar wind just prior to the event, and this may have provided an impulsive energy source for the waveguide mode. This is the first time the signature of a particular waveguide mode harmonic has been observed by satellites which are widely spaced in the magnetosphere. Moreover, we present the first unambiguous observation of the downtail propagation of a waveguide mode. The observation also provides possible evidence of dispersion in the Earth's outer magnetospheric waveguide.

1. Introduction

Ultralow frequency (ULF) pulsations may be excited in the Earth's magnetosphere by the solar wind. Early theoretical work considered how Kelvin-Helmholtz surface waves propagating on the magnetopause could couple to Alfvén resonances situated deep in the magnetosphere [*Chen and Hasegawa*, 1974; *Southwood*, 1974]. Following observations by *Kivelson et al.* [1984] of a compressional ULF wave disturbance with constant frequency over a range of L shells, the theory was refined to consider how the magnetosphere could act as a resonant cavity when perturbed by sudden impulses or density enhancements in the solar wind [*Kivelson and Southwood*, 1985, 1986]. Further theoretical developments produced the waveguide model in which the magnetosphere is open downtail, allowing fast mode energy to propagate antisunwards down the waveguide [*Walker et al.*, 1992; *Samson et al.*, 1992; *Harrold and Samson*, 1992; *Wright*, 1994].

Observational searches in the magnetosphere for the compressional cavity or waveguide modes believed to be responsible for driving field line resonances have been generally unsuccessful. Observations by *Crowley et al.* [1987, 1989] using the European Incoherent Scatter (EISCAT) radar determined the local ionospheric conductivity at the position of a field line resonance. They calculated a theoretical damping rate for the waves based on the observed conductivity; this theoretical damping rate was much greater than the observed wave damping. *Crowley et al.* [1987] argued that this was evidence that the field line resonance was being continually driven by a cavity mode, although the cavity mode itself was not observed directly. Very recently, *Yeo-*

[1]Now at Department of Physics, University of Alberta, Edmonton, Alberta, Canada.

[2]Now at Space Sciences Laboratory, University of California, Berkeley.

Paper number 97JA03175.
0148-0227/98/97JA-03175$09.00

man et al. [1997] used the Co-operative UK Twin Located Auroral Sounding System (CUTLASS) radar to observe the time-dependent evolution of a field line resonance. The evolution observed was in accord with the time-dependent cavity mode modelling of *Mann et al.* [1995]. *Yeoman et al.* [1997] argued that their observation represented a field line resonance being driven by a cavity mode, the cavity mode itself resulting from the impulsive excitation of the magnetosphere by a sudden impulse in the solar wind.

Observational searches for cavity modes using satellites *in situ* in the magnetosphere have generally concentrated upon looking for quasi-sinusoidal compressional oscillations with L-independent frequencies, or for enhancements in the Alfvén continuum at cavity mode eigenfrequencies. These cavity mode signatures were predicted by the modeling of *Lee and Lysak* [1989, 1991] in a dipole field geometry. Previous searches for these characteristics using the Active Magnetospheric Particle Tracer Explorers Charge Composition Explorer (AMPTE CCE) data set have been largely unsuccessful. When the satellite data are presented in the form of spectrograms [e.g., *Anderson et al.*, 1989, Plate 1], they do not show any evidence of compressional waves with constant frequencies over a range of L shells or of particular power enhancements in the Alfvén continuum [*Anderson et al.*, 1989; M.J. Engebretson and B.J. Anderson, The search for global mode ULF waves in the AMPTE CCE data set, submitted to *Journal of Geophysical Research*, 1995]. This may be the result of the low harmonics of cavity/waveguide modes typically having frequencies of a few millihertz (Pc5 waves) which are not well resolved by the AMPTE CCE spectrograms, the spectrograms typically being sensitive to waves with frequencies between 20 and 80 mHz [*Hughes*, 1994]. At these higher (Pc3-4) frequencies the eigenfrequencies of the three-dimensional magnetospheric cavity may be so closely packed so as to approach a continuum similar to that which is observed. Engebretson and Anderson also analyzed long periods of AMPTE CCE data, looking for Pc5 global cavity mode signatures with frequencies $\lesssim 10$ mHz. They found some evidence for slowly propagating (velocities ~ 100 km s^{-1}) compressional waves but no evidence for the expected L-independent cavity mode oscillations.

The absence of these monochromatic compressional wave signatures can be explained by inadequacies in the cavity model. If the outer magnetosphere behaves more like an open waveguide than a cavity, compressional wave energy will propagate downtail in a wave packet. In the waveguide model the decaying quasi-sinusoidal compressional cavity mode signatures are not expected. If a satellite observes a waveguide mode, it will only see oscillations for a finite time as the waves pass over it. Waveguide modeling has now put this on a firm theoretical footing [*Rickard and Wright*, 1994, 1995].

The waveguide model of *Rickard and Wright* [1995] has been used to successfully simulate the waves observed on the DE 1 satellite by *Lin et al.* [1992]; however, no observational studies to date have used multiple satellites to follow the tailwards propagation of a waveguide mode. In this paper we present observations of a suspected waveguide mode event from October 28, 1984. The event is observed in the magnetosphere near local noon by AMPTE CCE and in the local morning by AMPTE Ion Release Module (IRM) and UKS. The event is also seen at lower L shells by the ground-based magnetometers of the EISCAT magnetometer cross. We discuss the possible driving mechanisms for the waveguide mode and conclude that it was most probably impulsively driven by a solar wind sudden impulse incident upon the nose of the magnetosphere. We suggest that the dispersion observed during the event may be evidence that the Earth's outer magnetosphere acts as a waveguide for compressional ULF pulsations.

The paper is structured as follows: Section 2 presents the waveguide mode observations, section 3 presents a time of flight analysis of the downtail propagation of the mode and considers a possible impulsive energy source for the waves, section 4 considers waveguide mode theory and section 5 discusses the observed waveguide mode dispersion and compares it to the theoretical models. Finally, section 6 summarizes our paper.

2. Observations

Figure 1 shows the positions of the observations made by the satellites in the magnetosphere and by the magnetometers on the ground. The positions of AMPTE CCE and the twin AMPTE IRM/UKS satellites be-

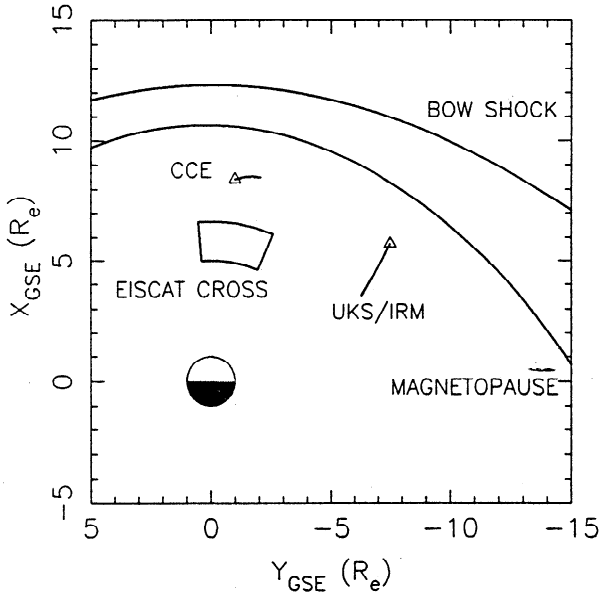

Figure 1. The positions of AMPTE CCE and AMPTE IRM/UKS at the time of the event mapped into the GSE X-Y plane. The solid lines represent the paths of the satellites between 0900 and 1030 UT and the symbol represents its position at 1030 UT. The field of view of the EISCAT magnetometer cross mapped into the GSE X-Y plane is also shown, as is the position of a model magnetopause and bow shock.

Table 1. Coordinates and L Shell Values of the EISCAT Magnetometer Cross Stations

Station	Code	Geographic		Geomagnetic		L Shell
		Latitude	Longitude	Latitude	Longitude	
Soroya	SOR	70.54	22.22	67.01	106.91	6.66
Alta	ALT	69.86	22.96	66.28	106.83	6.28
Kevo	KEV	69.76	27.01	65.95	109.82	6.12
Kilpisjarvi	KIL	69.05	20.70	65.61	104.41	5.96
Kautokeino	KAU	69.02	23.05	65.43	106.17	5.88
Muonio	MUO	68.01	23.53	64.39	105.73	5.44
Pello	PEL	66.90	24.08	63.23	105.34	5.01

All values were calculated using the International Geomagnetic Reference Field for 1987 at an altitude of 120 km.

tween 0900 and 1030 UT on October 28, 1984, are shown as solid lines; the overplotted triangles represent the satellite positions at the end of the interval at 1030 UT. As is clearly shown, IRM/UKS are outbound in the morning sector of the magnetosphere, whilst CCE remains on nearly constant L shells as it travels toward the local afternoon. The CCE and IRM/UKS satellites are separated by 6.2 R_E in the GSE X-Y plane at 0915 UT at the beginning of the event; the separation gradually increasing with time. This large separation is used later in the paper to analyze the downtail propagation of the waveguide mode. Also plotted as a small angular section in Figure 1 are the equivalent GSE X and Y range of the EISCAT magnetometer cross stations [*Lühr et al.*, 1984] between 0900 and 1030 UT mapped into the equatorial plane. The geographic and geomagnetic locations of the EISCAT magnetometer cross stations are given in Table 1. The ground-based magnetometers sample waves from a similar magnetic local time to AMPTE CCE but from lower L shells. Since the field of view of the magnetometers rotates with the Earth, the magnetometers observe waves from a small range of magnetic local time. Figure 1 also contains a model magnetopause [*Fairfield*, 1971] calibrated by an AMPTE UKS magnetopause crossing recorded later on the same day. A model bow shock position is also included.

2.1. AMPTE CCE and IRM/UKS Observations

In Figure 2 we present magnetic field variations observed by AMPTE CCE (thin line) and AMPTE UKS (thick line) between 0900 and 1030 UT on October 28, 1984. On the timescale of the waves we are interested in, the AMPTE UKS and IRM data sets are almost indistinguishable, and so we do not attempt any correlative studies between them. We plot the AMPTE UKS data in preference to the AMPTE IRM data in the remainder of this paper. The Pc5 event which forms the subject for the paper is observed as a series of about five or six cycles of compressional wave activity between 0915 and 1000 UT; similar wave activity being seen at both CCE and UKS. The oscillations at UKS occur slightly later than at CCE, which we attribute to the downtail propagation of the waveguide mode. This is especially clear in the B_x component between 0925 and 0945 UT, and in $|B|$ between 0930 and 0945 UT. The waves at both satellites have a period of about 380 s and are strongly compressional. This is consistent with the characteristics expected of a compressional waveguide mode.

2.2. EISCAT Magnetometer Cross Observations

In Figure 3 we plot the X (geographic north-south) and Y (geographic east-west) magnetic field variations as observed by the EISCAT magnetometer cross between 0900 and 1030 UT (note that there is no X component data available from the station KEV during this interval). A wave with very similar characteristics to those observed by the AMPTE satellites is seen

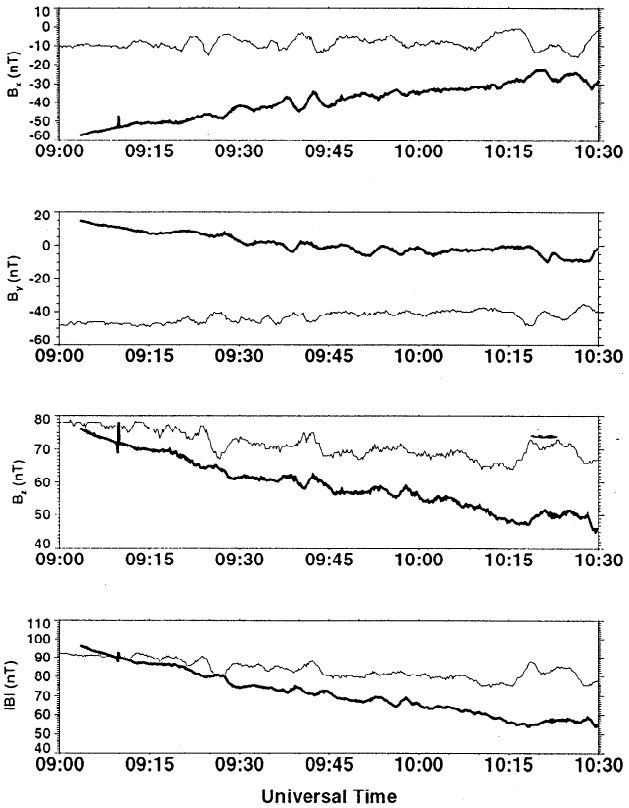

Figure 2. AMPTE CCE (solid line) and AMPTE UKS (bold line) GSE magnetic field components B_x, B_y, B_z and magnitude $|B|$ as a function of UT.

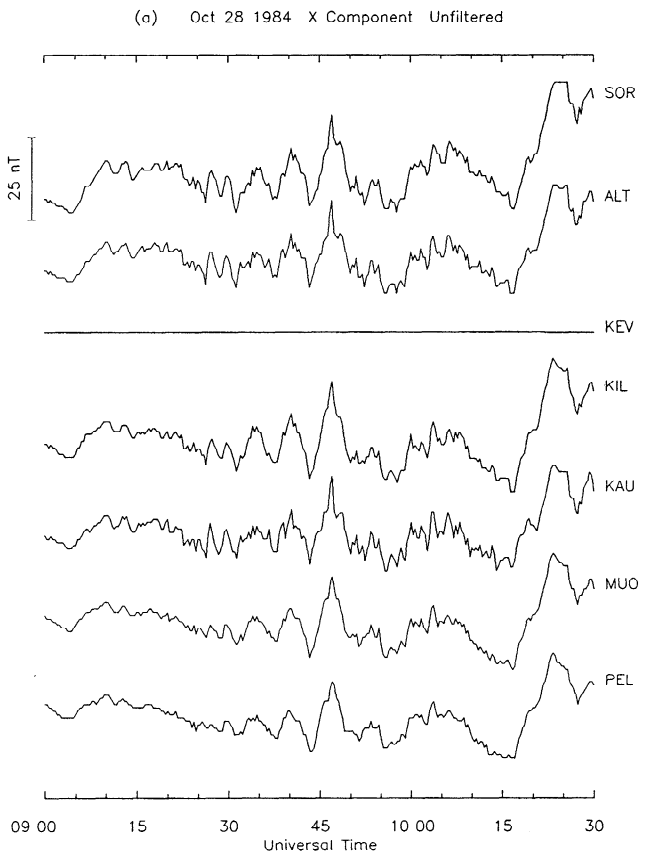

Figure 3. Unfiltered (a) X component and (b) Y component data from the EISCAT magnetometer cross.

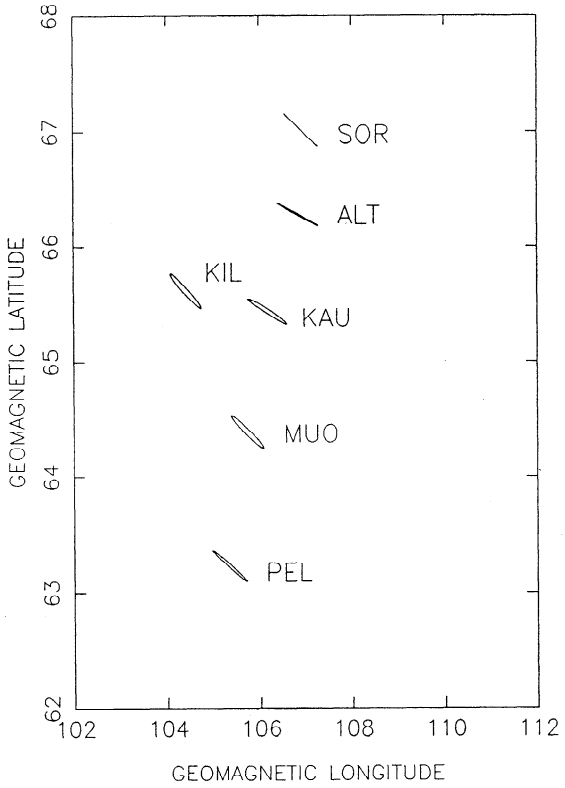

Figure 4. Polarization map displaying the wave polarization variation across the EISCAT magnetometer cross for the central period of the event. There is no ellipse for KEV because of a data gap in the X component.

by the ground-based magnetometers. The wave has a dominant period of 380 s, lasts for about five cycles, and is observed in both the X and Y components between 0925 and 1000 UT. We have used the technique of complex demodulation [*Beamish et al.*, 1979] to determine the amplitude, phase and polarization characteristics of the wave at the ground magnetometer stations. This technique is based on the fast Fourier transform and uses the dominant frequency component in a wave packet, in this case 2.6 mHz (corresponding to the dominant spectral component at 380 s), to estimate the average amplitude and polarization characteristics for the event at each station. The complex demodulation analysis shows that both the X and Y components have almost no latitudinal amplitude variation, the wave having a near constant amplitude across the entire array. In Figure 4 we present the resultant polarization ellipses as a function of the geomagnetic latitude and longitude of the observing magnetometer stations. The wave polarizations at all the stations have approximately the same orientation, pointing into the northwest quadrant (viewed in the direction of the ambient magnetic field). The polarization ellipticity is almost constant across the array, displaying only a slight tendency toward linear polarization at higher latitudes. The polarization sense at every station was anticlockwise when viewed in the direction of the ambient magnetic field.

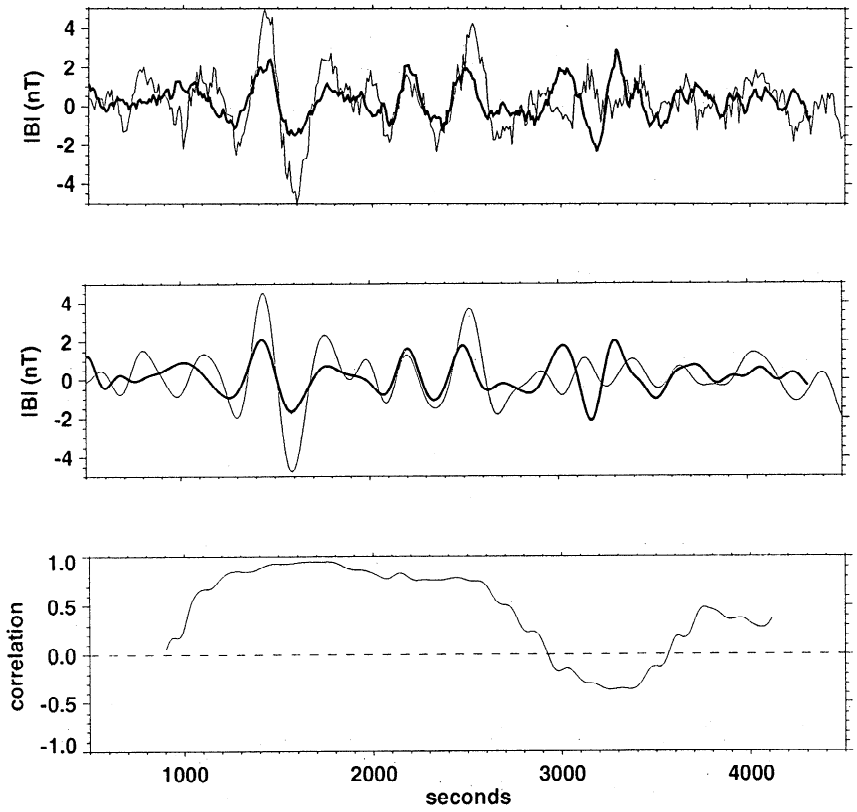

Figure 5. Magnetic field data from AMPTE CCE (thin line) and AMPTE UKS (thick line) as a function of time. Plotted are (top) the unfiltered magnetic field magnitudes $|\mathbf{B}|$, (middle) the band-pass filtered $|\mathbf{B}|$, and (bottom) the cross correlation between the two filtered data sets. The time axis shows seconds since 0900 UT, with the UKS data having been shifted forward by 180 s.

The EISCAT magnetometer cross data presented in Figures 3 and 4 show no evidence of a field line resonance, either in terms of any tendency toward a maximum wave amplitude on a particular field line, or of the possibility of a polarization reversal. It is possible, however, that a field line resonance is occurring at higher latitudes and that we are observing the lower latitude wave signature equatorward of the resonant field line. The observation that the waves have an anticlockwise polarization sense would be consistent with this interpretation (for westward propagating waves). We return to this possibility in the context of magnetospheric waveguide theory in section 5.

An attempt has also been made to estimate the m value (azimuthal wavenumber) of the disturbance using the phase differences measured between the Y components of the disturbance at the longitudinally spaced stations KIL, KAU and KEV. Unfortunately, because of the proximity of the stations, the phase differences between the stations were very small, making an accurate determination of the m values of the waves difficult. However, the results suggest that the m values for the waves are small ($|m| < 5$). This is important when considering the likely azimuthal wavenumber composition of the waveguide modes later in the paper.

3. Downtail Propagation of the Waveguide Mode

As we discussed previously, a slight time delay exists between the wave cycles observed at CCE and those observed at UKS. In this section we complete a more detailed analysis of this apparent tailward propagation. In Figure 5 we compare the magnetic field magnitudes $|\mathbf{B}|$ from CCE (thin line) and UKS (thick line) as a function of time in seconds since 0900 UT. The top panel shows the raw data, whilst in the middle panel the data have been band-pass filtered (between 1.5 and 6.25 mHz (approximately 160 s to 660 s)) to remove the trend of the background magnetic field variations and the higher frequency wave components. We have shifted the UKS data forward in time by 180 s to highlight the correlation with the CCE data. This shift was chosen to obtain the maximum correlation between the two wave trains for the early (large amplitude) wave cycles. Using an 800 s sliding window, we calculated the cross correlation between the filtered waveforms as a function of time and show this in the bottom panel of Figure 5. The degree of correlation between the two time series for the three to four large-amplitude wave cycles at the start of the wave packet is quite remarkable, especially considering

that CCE and UKS are separated by $\sim 6.2\ R_E$ (in the GSE X-Y plane). For later wave cycles, the correlation between the two satellites is greatly reduced; the waves displaying more complex and less quasi-sinusoidal signatures. The correlation between about 1200 and 2700 s is very significant, approaching unity for the majority of the interval. At later times in the time interval presented the correlation decreases. It is possible that this could be a result of the waveguide mode dispersing between the two observations, although some decrease in correlation could occur because of the satellite motion. The UKS data suggest the possible existence of some higher frequency components later in the wave packet which are not apparent at CCE. The amplitude of the waves is also less at UKS than at CCE. We interpret these features as properties of a propagating and dispersing waveguide mode in section 5.

We believe that the large degree of correlation which exists once the UKS data have been shifted by 180 s can be explained in terms of the time of flight of the leading edge of the waveguide mode wavepacket from CCE (situated near local noon) to UKS (situated in the local morning). If we assume that the group velocity of the waveguide mode is approximately aligned with the spacecraft separation vector, we can estimate the group velocity of the waveguide mode. Using the positions of the satellites at 0915 UT (at the beginning of the most coherent part of the wave packet), we calculate a group velocity (in the GSE X-Y plane) of 219 km s^{-1}. It is important to compare this group velocity with other typical wave speeds in the magnetosphere and magnetosheath and to establish the likely mechanism responsible for driving the waves.

In Figure 6 we display the magnitude of the ion flow velocity, the local Alfvén speed, and the background magnetic field measured on the out-bound trajectory of AMPTE UKS. To calculate the Alfvén speed we have used the observed magnetic field magnitudes and estimated the plasma density using the ion species composition observations of *Young et al.* [1982]. The prevailing K_p at the time of our event is $\sim 2o$ to $3-$, which suggests that the number density ratio O+/H+ ~ 0.4 (i.e., approximately 30% O+ and 70% H+) [*Young et al.*, 1982, Figure 12c]. Assuming quasi-neutrality, the electron density measurements from UKS were then used to estimate the plasma mass density, resulting in the Alfvén speed profile shown in the middle panel of Figure 6.

In the time interval presented in Figure 6, the UKS satellite travels toward higher L shells in the magnetosphere until it crosses the magnetopause at about 1220 UT. The compressional waveguide mode event can be clearly seen in the raw magnetic field data between 0915 and 1000 UT. In the magnetosheath the flow speed rises from $\sim$ 160 km s^{-1} at the magnetopause boundary to $\sim$ 190 km s^{-1} at 1400 UT. It is possible that the compressional waves could be the magnetospheric signature of a plasma disturbance in the magnetosheath; the compression of the magnetopause by the disturbance being observed as compressional waves in the magnetosphere.

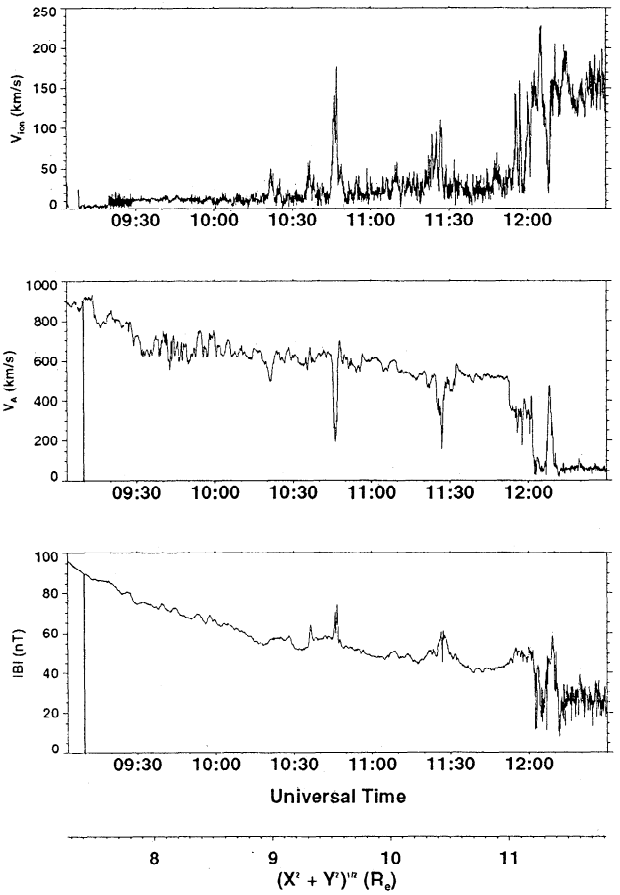

Figure 6. Ion velocity ($V_{\rm ion}$), Alfvén speed (V_A), and total magnetic field magnitude ($|\mathbf{B}|$) observed by UKS as a function of UT.

However, we do not favor this as the likely source of the waves because the flow speeds observed by UKS in the magnetosheath appear to be too slow to account for the observed time of flight between CCE and UKS. This scenario is made even more unlikely since the magnetosheath flow speed near the stagnation point will be very small (see, for example, the magnetosheath modeling of *Spreiter and Stahara* [1980]). The average magnetosheath flow speed between the local times of CCE and UKS will consequently be much less than that measured by UKS in the local morning at 0900 MLT, and this makes agreement between an average magnetosheath flow speed and the wave's time of flight even more difficult to reconcile.

It is also possible that the disturbance was the magnetospheric signature of a Kelvin-Helmholtz (KH) surface wave propagating along the magnetopause. However, calculations by *Walker* [1981] using a finite thickness magnetopause suggest that the fastest growing KH waves will have a tailwards wavelength (λ) $\sim$ 10 times the thickness of the boundary layer; the period of the KH waves being given by $T \sim \lambda/V_0$, where V_0 is half the magnetosheath flow speed [*Walker*, 1981]. The thickness of the low-latitude boundary layer is generally a few hundred kilometers at the subsolar magnetopause and

rises to $\sim 1\ R_E$ on the flanks [*Yumoto and Saito*, 1980]. Using $V_0 = 100$ km s^{-1} (approximately half the magnetosheath flow speed observed by UKS) produces a period ~ 30 s near the subsolar magnetosphere (assuming a width of 300 km) and a period ~ 640 s on the flanks, the predicted period at the nose being much lower than that observed. This suggests that KH surface waves are not a likely source of Pc5 waves near the subsolar point. It is possible, however, that Pc5 waves further down the flanks are driven by the Kelvin-Helmholtz mechanism. KH waves are more unstable there [e.g., *Miura*, 1992], and this is where Pc5 field line resonances (FLRs) are most frequently observed [see, e.g., *Cao et al.*, 1994].

We believe that the most likely driving source of the observed compressional Pc5 waves is impulsive variations in the solar wind. These impulses are likely to have scale sizes greater than the magnetosphere and can excite the entire magnetospheric cavity. The impulses drive waveguide modes in the magnetosphere which subsequently propagate tailwards. Modes with low azimuthal wavenumbers (m values) will have group velocities much lower than the local Alfvén speed [see, e.g., *Wright*, 1994]. In Figure 6 (middle panel) the Alfvén speed can be seen to decrease with increasing L shells but remains very much greater than the calculated wave group speed of ~ 220 km s^{-1}. We believe that the waves we see are the signature of a waveguide mode, and we discuss this possibility in detail in the next section.

To look for a possible signature of a solar wind source for the waveguide mode, we examined data from the IMP 8 satellite which was situated upstream of the Earth. Prior to the onset of the wave event, IMP 8 saw an enhancement in solar wind ram pressure of about 30%. Unfortunately, there is a large data gap immediately following the ram pressure enhancement which covers the entire interval of the event. Much later, when data coverage resumed, the ram pressure had returned to its previous value. We suggest that this could represent the solar wind driver of the waveguide mode, but the data gap prevents us testing this hypothesis further.

4. Waveguide Mode Theory

The theoretical details of compressional MHD wave propagation in a model magnetospheric waveguide have been developed by *Wright* [1994]. In Wright's model a Cartesian geometry is used: the background magnetic field is uniform and lies in the $\hat{\mathbf{z}}$ direction, a density profile $\rho(x)$ is prescribed in the $\hat{\mathbf{x}}$ direction to represent a monotonically decreasing radial Alfvén speed profile, and the waveguide is uniform in the tailwards ($\hat{\mathbf{y}}$) direction. The wave source acts near $y = 0$, with the subsequent tailwards wave propagation being examined as a function of x, y and time. This waveguide is illustrated schematically in Figure 7.

Waves in this waveguide can be described in the WKB limit by [*Inhester*, 1987; *Wright*, 1994]

$$\frac{d^2 b_z}{dx^2} + \left(\frac{\omega^2}{v_A^2(x)} - k_y^2 - k_z^2 \right) b_z = 0. \qquad (1)$$

The effective radial wavenumber of the waves is given by

$$k_x^2(x,\omega) = \frac{\omega^2}{v_A^2(x)} - k_y^2 - k_z^2 \qquad (2)$$

so that the wave's turning point (where $k_x^2 = 0$) is a function of both the wave frequency ω and k_y (k_z is assumed to be fixed by considering a single field-aligned harmonic). Equation (1) can be used to calculate the ray trajectories for the k_y components of a particular wave packet: a schematic of the refraction of three typical rays having wavenumbers k_{yn} ($n = 1, 2, 3$) are also shown in Figure 7 (adapted from *Wright* [1994]). Each ray penetrates to a different turning point x_n (x_0 is the turning point for waves with $k_y = 0$). Similarly, each mode propagates down the waveguide with different group speeds v_{gn}, traveling a distance $y = v_{gn}t$ in a time t. In general, waves with larger k_y have trajectories which remain close to the magnetopause (i.e., near x_m) in the region of the lowest Alfvén speed, whereas lower k_y modes have rays initially directed more per-

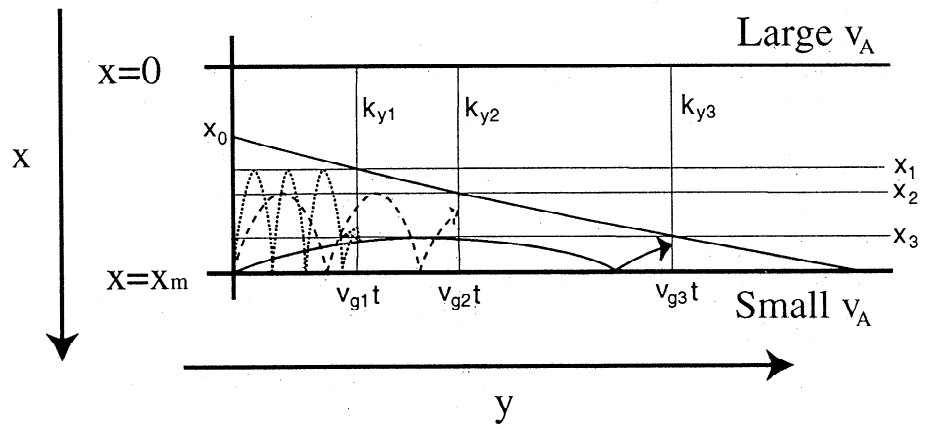

Figure 7. Schematic diagram of the Earth's magnetospheric waveguide, including the ray trajectories for tailwards propagating waveguide modes with three different k_y values (k_{yn}, $n = 1, 2, 3$). Each ray penetrates to a different turning point x_n and propagates a distance $y_n = v_{gn}t$ in a time t since the modes were excited. Adapted from *Wright* [1994].

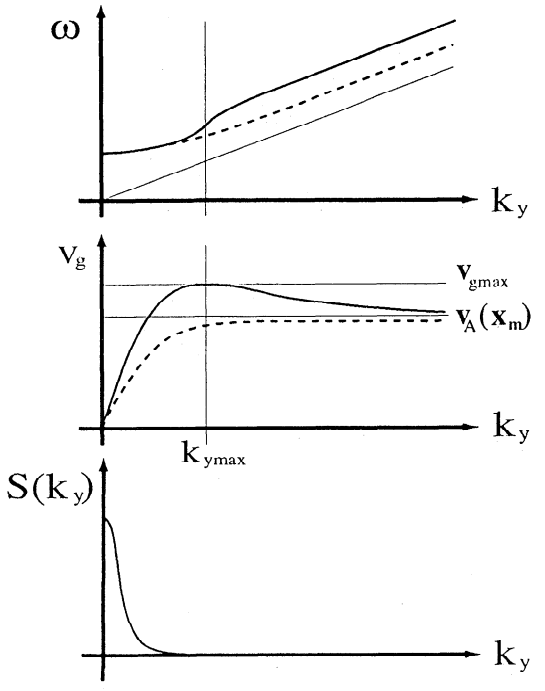

Figure 8. Schematic diagrams of (top) waveguide mode $\omega - k_y$ dispersion, (middle) waveguide mode group velocity as a function of k_y, and (bottom) a possible spectrum $S(k_y)$ of waveguide modes driven by a solar wind impulse incident upon the magnetosphere. In the first two panels dashed lines represent the behavior in a uniform waveguide, whilst the solid lines represent that in a nonuniform waveguide. Adapted from *Wright* [1994].

pendicular to the waveguide and penetrate deeper into the magnetosphere. Consequently, the waveguide generates spatial k_y dispersion in the $\hat{\mathbf{x}}$ direction. The k_y value corresponding to the fastest $\hat{\mathbf{y}}$ group velocity v_g $(= \partial\omega/\partial k_y)$ depends on the $\hat{\mathbf{x}}$ inhomogeneity in the waveguide. In a uniform waveguide, v_g increases monotonically with k_y. This is the case we have illustrated in Figure 7 whereby the modes with higher values of k_{yn} possess larger values of x_n and larger v_{gn}. Consequently, the mode which propagates fastest down the waveguide has the largest k_y. However, in a nonuniform waveguide with a monotonically decreasing Alfvén speed there can be an intermediate k_y which maximizes v_g. This can occur because waves with lower k_y can have a ray which samples an enhanced average v_A between its turning point and x_m. For certain lower k_y values this can compensate for the additional path length accrued from rays penetrating deeper into the magnetosphere and generate a local v_g maximum at a particular value of k_y.

In both the uniform and nonuniform waveguides, waves with $k_y = 0$ have $v_g = 0$, and waves with $k_y \to \infty$ have $v_g \to v_A(x_m)$. The temporal dispersion seen by an observer downtail from $y = 0$ will consequently depend upon the plasma profiles of the waveguide. In the first and second panels of Figure 8 we show schematic profiles of waveguide mode dispersion and group velocity as a function of k_y for both uniform (dashed line) and nonuniform (solid line) radial Alfvén speed profiles. The differing dispersion and group velocity characteristics are clearly shown. In the nonuniform waveguide the waves with maximum group speed ($v_{g\max}$) clearly have an intermediate wavenumber $k_{y\max}$, with $k_{y\max}$ representing the position where the $\omega - k_y$ diagram has maximum gradient. We now consider our observations in the light of this theory.

5. Dispersion in the Earth's Magnetospheric Waveguide

As discussed in section 3, it is likely that the energy source for the observed waveguide mode was a large-scale structure (possibly a density enhancement) in the solar wind. The character of the observable magnetospheric response to this disturbance will depend upon the k_y spectrum which it excites, and on the subsequent dispersion and propagation of the waves in the waveguide. If the wave front of this disturbance is almost planar on the scale size of the magnetosphere, the k_y spectrum of the waves excited will be dominated by low k_y components. If we consider this disturbing impulse to have a scale of ΔY on the magnetopause, the dominant m value for a magnetosphere with a standoff distance of L_{mp} would be $m = 2\pi L_{mp} R_E/\Delta Y$. For example, assuming a typical $\Delta Y \sim 10\ R_E$ and a standoff distance of $10\ R_E$ gives a typical $m \sim 2\pi$. Pc5 field line resonances are generally observed to have $m \lesssim 10$, which is consistent with the above theoretical estimate and also consistent with the m value inferred for our event from the ground-based observations. A sudden impulse with a large scale-size would be unlikely to drive any very high k_y modes, and hence we anticipate that the resulting waveguide mode spectrum $S(k_y)$ will be cut off toward large k_y. As we discussed earlier, the group velocity of the leading edge of the waveguide mode wave packet travels at a speed much less than the Alfvén speed at the magnetopause (the lowest speed in the waveguide). This also suggests that $S(k_y)$ only contains a narrow band of the very smallest k_y components; the group velocity of the largest k_y part of the spectrum $S(k_y)$ excited in the magnetosphere clearly being much less than the asymptotic ($k_y \to \infty$) group speed (since the observed $v_g \ll v_g(k_y \to \infty) = v_A(x_m)$). A possible spectrum $S(k_y)$ is schematically illustrated in the bottom panel of Figure 8.

The details of whether the cutoff occurs before or after any possible v_g peak in the k_y spectrum will critically depend on the details of the radial Alfvén speed profile in the waveguide. In all cases the wave component with maximum v_g will be seen first by an observer situated down the waveguide. If $S(k_y)$ cuts off before the peak in v_g, the highest k_y components will arrive first in both the uniform and nonuniform waveguide scenarios. In that case it is not possible to observationally distinguish between uniform and nonuniform waveguide behavior. We believe that this is probably the case for our event. If on the other hand $S(k_y)$ includes the group

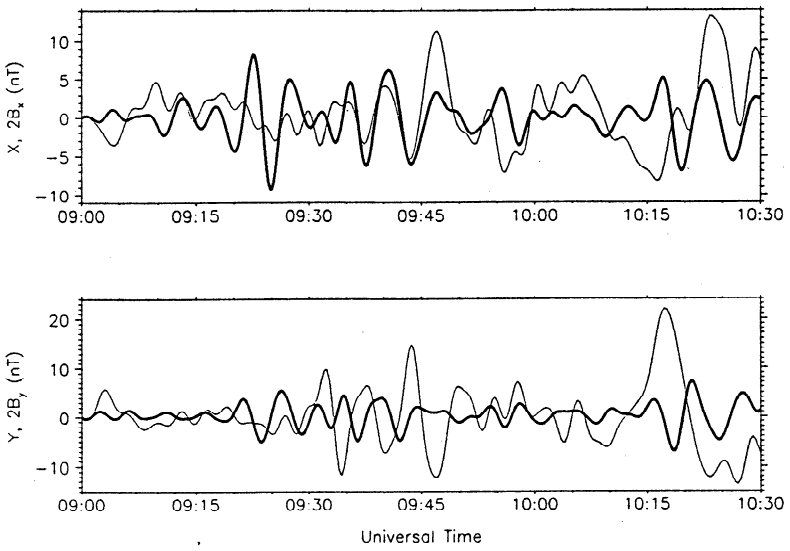

Figure 9. Band-pass filtered AMPTE CCE magnetic field components B_x and B_y (thick lines) overplotted with the KAU X and Y components (thin line). The ground magnetometer data have been filtered with the same band pass, and the amplitudes of the satellite data have been doubled to enable an easier comparison between the ground-based and the magnetospheric data.

speed peak, intermediate k_y components would arrive first, followed by a superposition of waves with k_y on either side of the group speed peak, and finally by a monochromatic signal comprised of only the lowest k_y components (see, for example, the modeling signatures of [*Rickard and Wright*, 1994, Figure 7]).

Detailed examination of Figure 5 suggests the possible development of higher frequency wave components in the UKS data later in the wave packet at about 1000 UT. These higher frequency components are not apparent in the CCE data. If these features occur as a result of waveguide mode dispersion, it would seem likely that they are due to spatial rather than temporal dispersion. This could result from UKS sampling fields closer to the magnetopause later in the wave packet and consequently revealing the structure of those (higher) k_y components which are trapped nearer to the magnetopause and whose turning points lie outside the position of UKS (and CCE) at the start of the wave packet. If this were the case it would require the solar wind driver to act over finite time so that these higher k_y components are still present when UKS observes them on higher L shells later in the wave packet. The suggestion that these features occur as the result of waveguide mode spatial dispersion is tentative but is a possible explanation of the observations.

A more interesting and striking feature of Figure 5 is the decay in amplitude of the waveforms at the leading edge of the wave packet as it propagates from CCE to IRM/UKS. In a dispersive waveguide, the amplitude of a wave propagating down the waveguide will decrease as the wave energy is spread over a larger volume. Hence dispersion leads to a decay in wave energy density as it propagates down a waveguide. The amplitude of the waveform at UKS is much smaller than that at CCE, consistent with this dispersion. In addition to this decay in energy density, energy can also be lost from the waveguide mode wave packet via a variety of loss mechanisms. Energy losses can result from imperfect reflection at the boundaries of the guide, from direct ionospheric dissipation (expected to be small for dominantly compressional waves [*Kivelson and Southwood*, 1988]) or from the waveguide mode driving a field line resonance. From Figure 7, we calculated the total compressional energy in each of the wave packets observed by CCE and by UKS. The total energy in the wave packet observed by UKS is only 38% of the energy in the wave packet observed by CCE, which suggests that a considerable amount of waveguide mode energy has been lost from the waves between the two observations.

To examine the possibility that the waveguide mode excites a field line resonance, we compare in Figure 9 the band-pass filtered CCE B_x and B_y magnetic field components from Figure 5 (thick lines) with the X and Y variations from the ground station KAU (also band passed with the same filter; thin lines). Note that the amplitudes of the CCE data have been doubled to enable an easier comparison with the ground-based data. Both of these observations are made at almost the same local time but on differing L shells (see Figure 1). The dominant wave oscillations within this frequency band have the same period, but the phase relationship from the satellite to the ground appears complex. The ground-based data also appear to contain more high-frequency components than the satellite data. Both of these features may be due to the spatial integration inherent in ground-based magnetometer observations or it could be a result of signal modifications due to ionospheric currents which can make the direct comparsion of ground and satellite data difficult.

Throughout this interval the wave observed in the ground-based data has an anti-clockwise polarization

sense. The B_x and B_y components at CCE, on higher L shells, are almost in quadrature; however, the wave here also has an anticlockwise polarization, and hence there appears to be no polarization reversal between the observations (i.e., the resonant field line does not appear to be between the two observations). Typically, the amplitude of a FLR maximizes at the resonant field line where the toroidal component exhibits a phase change of π over radial distances $\sim 2\ R_E$ [e.g., *Ziesolleck and McDiarmid*, 1994, Figure 7]. The CCE and EISCAT magnetometer cross observations show no evidence of a polarization reversal, so it is unlikely that a resonance exists at this local time on the L shells between CCE and EISCAT. However, a FLR polarization reversal should only exist at those local times where a resonant response is being driven. Local time localized resonant signatures of this kind were produced by the waveguide modeling of *Rickard and Wright*, [1995, Figure 6], so it is possible that a field line resonance could be being driven at earlier (later) local times away from noon and toward dawn (dusk).

To make more detailed comparisons between the polarizations of the waves observed by the EISCAT magnetometers and by AMPTE CCE, we need to consider the effect of the ionosphere. The polarization sense of waves is unaffected by transmission through the ionosphere; however, the orientations of the polarization ellipses can be significantly altered. Purely Alfvénic waves are subject to a polarization rotation of 90° [e.g., *Hughes*, 1974]; however, fast waves are relatively unaffected by the ionosphere [*Kivelson and Southwood*, 1988]. In reality, fast and Alfvén waves are coupled together in the magnetosphere so that the effect of transmission through the ionosphere to the ground will depend on the location of the observation; close to the resonance the waves should be dominantly Alfvénic, whilst far from the resonance they will be dominated by their fast mode component. This makes comparison between the ground and satellite data very difficult, especially as the ground magnetometers observe a spatially integrated signal [*Poulter and Allan*, 1985]. In the case of a cavity/waveguide mode, this situation is complicated further by the possible existence of polarization reversals in latitude due to the nodes and antinodes which can exist in the oscillatory part of the modes [*Allan et al.*, 1986; *Zhu and Kivelson*, 1988], so that the wave polarizations observed can be strongly dependent on the position of the observation.

Returning to Figure 9, between 0930 and 1000 UT there is a good "in phase" correlation between CCE B_x and KAU X (this interval also represents the part of the wave packet where maximum correlation exists between CCE and UKS after the time of flight shift of 180 s). The CCE B_y and KAU Y components, however, appear to be almost in antiphase, especially from around 0930 to 0940 UT. In general, between 0930 and 1000 UT, B_y and Y (if they show any correlation at all) appear to be between 90° and 180° out of phase with each other in the dominant spectral component (380 s). If the waveguide mode is a dominantly fast mode oscillation and the 90° polarization rotation is not operative, then the differences in phase could be the result of the radial oscillatory structure of the waveguide mode. We believe that this is the most likely explanation for the phase differences, especially since there is no other evidence which supports the existence of a FLR at the local time of CCE and the EISCAT magnetometer cross.

The constant nature of the phase and ellipticity of the waves observed on the ground (Figure 4) is consistent with the known behavior well equatorwards of a field line resonance [e.g., *Ziesolleck and McDiarmid*, 1994; *Chisham and Orr*, 1997]. If this is the signature of the radially evanescent part of the waveguide mode then this suggests that the EISCAT magnetometer cross was probably equatorward of any resonance which might have been driven by the waveguide mode. We estimate that a 2.6 mHz resonance could lie at $L \sim 7.5$ by comparing with the resonance positions of 1.9 and 3.4 mHz Pc5 waves observed in the local morning by *Ziesolleck and McDiarmid*, [1994, Figure 6]. This is consistent with a resonance position on L shells between CCE and the EISCAT magnetometer cross. Our earlier arguments suggest that the resonance is probably not located at the same local time as CCE and EISCAT (around noon), so that if a FLR was being driven by the waveguide mode it would most likely be located at earlier (later) local times, that is, toward dawn (dusk). It is also possible that the waveguide mode did not drive a FLR and that the energy loss from its wave packet occurred as a result of other direct energy loss mechanisms. We have not observed any FLR characteristics directly, and so can only speculate about possible FLR existence at the locations not sampled by our instruments.

The observational features of the waveguide mode event can be summarized by the following scenario which is illustrated schematically in Figure 10. A sudden impulse in the solar wind passes through the bow shock and is incident upon the magnetopause. This impulsively excites waveguide modes with a low k_y spectrum in the magnetosphere near the subsolar point and these waves subsequently propagate down the waveguide (time t_0 in Figure 10). The largest k_y components in the wave packet ($k_y \sim 6$) propagate fastest down the waveguide but travel slower than the local magnetospheric Alfvén speed. The leading edge of the disturbance (largest k_y) decreases in amplitude as it propagates down the waveguide as a result of dispersion in the wave packet (causing a local decrease in the energy density of the waves). After ~ 180 s, the leading edge of this disturbance reaches AMPTE UKS (time t_1 in Figure 10). The lower k_y components penetrate deeper within the magnetosphere but propagate more slowly along the waveguide and stay closer to the subsolar point. These lower k_y waves remain on the same L shells for longer periods and in some cases can act as long-lived and coherent drivers for field line resonances [*Wright*, 1994]. The total compressional energy in the wave packet decays by a factor of 0.38 at UKS compared to that at CCE. This suggests that the waveguide

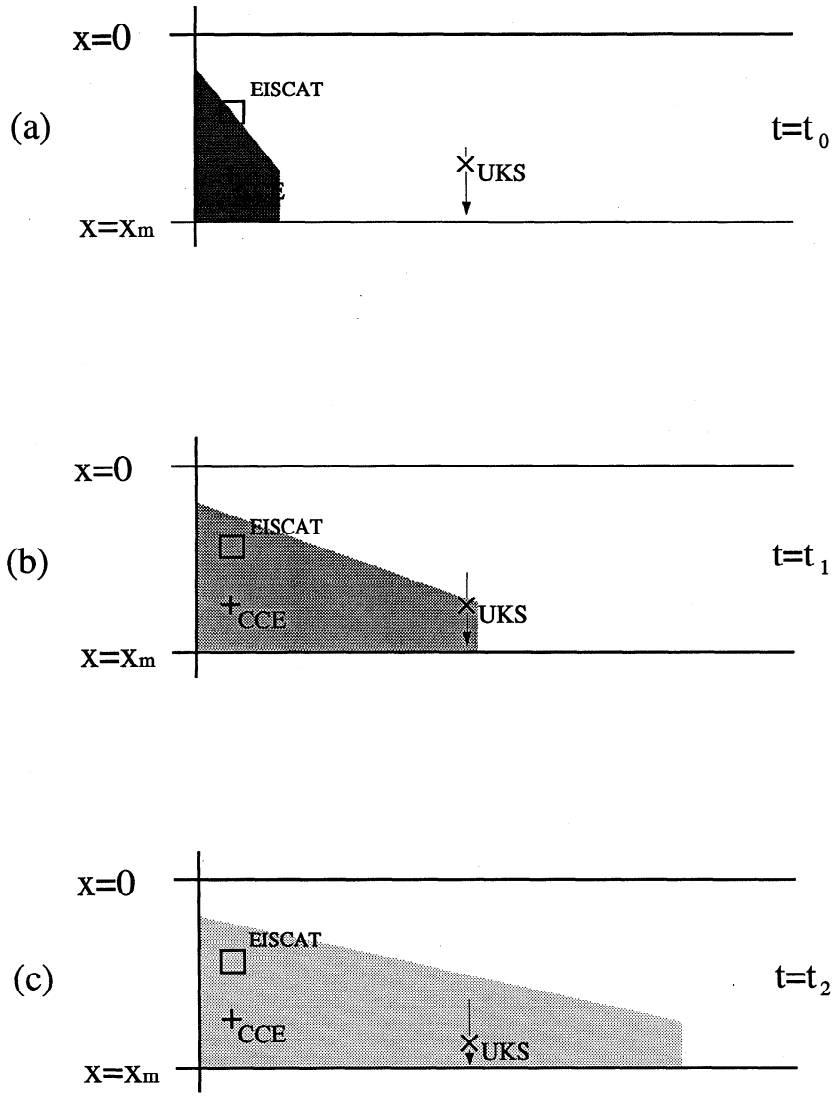

Figure 10. Schematic diagram of the tailwards propagation and evolution of the waveguide modes as a function of time. (a) Time t_0 shortly after the action of the sudden impulse, (b) time t_1 when the leading edge of the compressional waveguide mode reaches AMPTE UKS/IRM, and (c) time t_2 when the latter parts of the wave packet pass over UKS/IRM.

mode might have deposited energy into a field line resonance. At around 1000 UT (time t_2 in Figure 10) there is some indication of higher frequency components in the magnetic field data at UKS as it travels to higher L shells. This is possibly evidence of spatial dispersion in the Earth's magnetospheric waveguide resulting from the trapping of higher frequency (higher k_y) wave components nearer to the magnetopause.

6. Summary

In this paper we have presented the first multiple satellite observations of the downtail propagation of a Pc5 compressional magnetospheric waveguide mode. The wave is observed near local noon by AMPTE CCE and $\sim 6.2\ R_E$ away in the local morning by AMPTE IRM and UKS. It lasts for about five or six cycles in both data sets; the leading edge of the waveform displaying a remarkable coherence between CCE and IRM/UKS despite their large separation. The leading edge of the wave packet arrives at IRM/UKS about 180 s after it was observed at CCE, and this can be explained in terms of waveguide mode theory. The high coherence permits a time of flight analysis, revealing a waveguide mode tailwards group velocity $\sim$ 220 km s^{-1} (much less than the local magnetospheric Alfvén speeds). The ground-based signature of the wave is also seen by the EISCAT magnetometer cross, observing at the same local time as CCE but on lower L shells. The ground-based signature has the same frequency and lasts for the same number of cycles as the magnetospheric signature.

We have analyzed the event in detail in terms of the waveguide mode theory developed by *Wright* [1994]

and have concluded that there is some evidence for the waveguide mode dispersion predicted by the theory. Furthermore, we provide some evidence that the waveguide modes were excited by a sudden impulse in the solar wind and that this impulse excited magnetospheric waveguide modes with a spectrum dominated by low azimuthal wavenumber (m) components. Some of these low m modes may be driving a field line resonance on L shells between CCE and the EISCAT cross, but at a different local time. Interestingly, the frequency (2.6 mHz) of the waveguide mode is very close to one of the statistically significant frequencies (at 2.7 mHz) which appear to dominate the Pc5 pulsation spectra as observed in the ionosphere by HF radar [*Samson et al.*, 1991; *Walker et al.*, 1992], as well as by magnetometers on the ground [*Ziesolleck and McDiarmid*, 1994]. We believe that our event represents the magnetospheric signature of the oscillation of a particular radial harmonic of the outer magnetospheric waveguide.

Our observation is only present in the time series for about five cycles (only being observed as the waveguide mode passes over the satellite). We believe that this short wave train length may be one of the reasons that the detection of compressional waveguide mode signatures in spectrograms taken by satellites in the magnetosphere has proved so elusive. We believe that impulsively driven Pc5 waveguide modes, such as the one presented here, will be responsible for driving FLRs in the dayside magnetosphere near the subsolar point. Further careful searches in multisatellite data for these short wave train compressional wave signatures may well reveal the existence in the magnetosphere of the waveguide mode harmonics. Wavelet analysis techniques may be of use in searching for these temporally narrow (about five wave cycles) signatures.

Acknowledgments. I.R.M. was supported by PPARC grant GR/K94133, G.C. was supported by PPARC grant GR/J88388, and S.D.B. was supported in part by PPARC grants GR/L37748 and GR/L29347. The authors would like to thank Brian Anderson for supplying the AMPTE CCE data, and Ari Viljanen and Lasse Hakkinen for supplying the data from the EISCAT magnetometer cross. The EISCAT magnetometer project was a German-Finnish collaboration conducted by the Technical University of Braunschweig. AMPTE UKS ion and electron data for this study were provided by the UK STP data handling facility at DRAL, U.K. The AMPTE UKS magnetometer data was provided by Malcolm Dunlop at ICSTM and was obtained from the data center at DRAL, U.K. The authors thank Mike Hapgood, Alan Johnstone, and David Southwood for permission to use the AMPTE UKS data.

The Editor thanks W. Allan for his assistance in evaluating this paper.

References

Allan, W., S. P. White, and E. M. Poulter, Impulse-excited hydromagnetic cavity and field-line resonances in the magnetosphere, *Planet. Space Sci.*, *34*, 371, 1986.

Anderson, B. J., M. J. Engebretson, and L. J. Zanetti, Distortion effects in spacecraft observations of MHD toroidal standing waves: Theory and observations, *J. Geophys. Res.*, *94*, 13,425, 1989.

Beamish, D., H. W. Hanson, and D. C. Webb, Complex demodulation applied to Pi2 geomagnetic pulsations, *Geophys. J. R. Astron. Soc.*, *58*, 471, 1979.

Cao, M., R. L. McPherron, and C. T. Russell, Statistical study of ULF wave occurrence in the dayside magnetosphere, *J. Geophys. Res.*, *99*, 8731, 1994.

Chen, L., and A. Hasegawa, A theory of long-period magnetic pulsations 1. Steady state excitation of field line resonance, *J. Geophys. Res.*, *79*, 1024, 1974.

Chisham, G., and D. Orr, A statistical study of the local time asymmetry of Pc5 ULF wave characteristics observed at mid-latitudes by SAMNET, *J. Geophys. Res.*, *102*, 24,339, 1997.

Crowley, G., W. J. Hughes, and T. B. Jones, Observational evidence for cavity modes in the Earth's magnetosphere, *J. Geophys. Res.*, *92*, 12,233, 1987.

Crowley, G., W. J. Hughes, and T. B. Jones, Correction to "Observational evidence for cavity modes in the Earth's magnetosphere", *J. Geophys. Res.*, *94*, 1555, 1989.

Fairfield, D. H., Average and unusual locations of the Earth's magnetopause and bow shock, *J. Geophys. Res.*, *76*, 6700, 1971.

Harrold, B. G., and J. C. Samson, Standing ULF modes of the magnetosphere: A theory, *Geophys. Res. Lett.*, *19*, 1811, 1992.

Hughes, W. J., The effect of the atmosphere and ionosphere on magnetospheric micropulsation signals, *Nature*, *249*, 493, 1974.

Hughes, W. J., Magnetospheric ULF waves: A tutorial with a historical perspective, in *Solar Wind Sources of Magnetospheric Ultra-Low-Frequency Waves*, edited by M. J. Engebretson et al., vol. 81 of *Geophys. Monogr. Ser.*, pp. 1–11. AGU, Washington, D.C., 1994.

Inhester, B., Numerical modeling of hydromagnetic wave coupling in the magnetosphere, *J. Geophys. Res.*, *92*, 4751, 1987.

Kivelson, M. G., and D. J. Southwood, Resonant ULF waves: A new interpretation, *Geophys. Res. Lett.*, *12*, 49, 1985.

Kivelson, M. G., and D. J. Southwood, Coupling of global magnetospheric MHD eigenmodes to field line resonances, *J. Geophys. Res.*, *91*, 4345, 1986.

Kivelson, M. G., and D. J. Southwood, Hydromagnetic waves and the ionosphere, *Geophys. Res. Lett.*, *15*, 1271, 1988.

Kivelson, M. G., J. Etcheto, and J. G. Trotignon, Global compressional oscillations of the terrestrial magnetosphere: The evidence and a model, *J. Geophys. Res.*, *89*, 9851, 1984.

Lee, D. H., and R. L. Lysak, Magnetospheric ULF wave coupling in the dipole model: The impulsive excitation, *J. Geophys. Res.*, *94*, 17,097, 1989.

Lee, D. H., and R. L. Lysak, Impulsive excitation of ULF waves in the three-dimensional dipole model: The initial results, *J. Geophys. Res.*, *96*, 3479, 1991.

Lin, N., M. J. Engebretson, L. A. Reinleitner, J. V. Olson, D. L. Gallagher, L. J. Cahill Jr., J. A. Slavin, and A. M. Persoon, Field and thermal plasma observations of ULF pulsations during a magnetically disturbed interval, *J. Geophys. Res.*, *97*, 14,859, 1992.

Lühr, H., S. Thurey, and N. Klocker, The EISCAT-magnetometer cross. Operational aspects: First results, *Geophys. Surv.*, *6*, 305, 1984.

Mann, I. R., A. N. Wright, and P. S. Cally, Coupling of magnetospheric cavity modes to field line resonances: A study of resonance widths, *J. Geophys. Res.*, *100*, 19,441, 1995.

Miura, A., Kelvin-Helmholtz instability at the magne-

topause boundary: Dependence on the magnetosheath sonic Mach number, *J. Geophys. Res.*, *97*, 10,655, 1992.

Poulter, E. M., and W. Allan, Transient ULF pulsation decay rates observed by ground based magnetometers: The contribution of spatial integration, *Planet. Space Sci.*, *33*, 607, 1985.

Rickard, G. J., and A. N. Wright, Alfvén resonance excitation and fast wave propagation in magnetospheric waveguides, *J. Geophys. Res.*, *99*, 13,455, 1994.

Rickard, G. J., and A. N. Wright, ULF pulsations in a magnetospheric waveguide: Comparison of real and simulated satellite data, *J. Geophys. Res.*, *100*, 3531, 1995.

Samson, J. C., R. A. Greenwald, J. M. Ruohoniemi, T. J. Hughes, and D. D. Wallis, Magnetometer and radar observations of magnetohydrodynamic cavity modes in the Earth's magnetosphere, *Can. J. Phys.*, *69*, 929, 1991.

Samson, J. C., B. G. Harrold, J. M. Ruohoniemi, and A. D. M. Walker, Field line resonances associated with MHD waveguides in the magnetosphere, *Geophys. Res. Lett.*, *19*, 441, 1992.

Southwood, D. J., Some features of field line resonances in the magnetosphere, *Planet. Space Sci.*, *22*, 483, 1974.

Spreiter, J. R., and S. S. Stahara, A new predictive model for determining solar wind-terrestrial planet interactions, *J. Geophys. Res.*, *85*, 6769, 1980.

Walker, A. D. M., The Kelvin-Helmholtz instability in the low-latitude boundary layer, *Planet. Space Sci.*, *829*, 1119, 1981.

Walker, A. D. M., J. M. Ruohoniemi, K. B. Baker, and R. A. Greenwald, Spatial and temporal behavior of ULF pulsations observed by the Goose Bay HF radar, *J. Geophys. Res.*, *97*, 12,187, 1992.

Wright, A. N., Dispersion and wave coupling in inhomogeneous MHD waveguides, *J. Geophys. Res.*, *99*, 159, 1994.

Yeoman, T. K., D. M. Wright, T. R. Robinson, J. A. Davies, and M. Rietveld, High spatial and temporal resolution observations of an impulse-driven field line resonance in radar backscatter artificially generated with the Tromso heater, *Ann. Geophysicae*, *15*, 634, 1997.

Young, D. T., H. Balsiger, and J. Geiss, Correlations of magnetospheric ion composition with geomagnetic and solar activity, *J. Geophys. Res.*, *87*, 9077, 1982.

Yumoto, K., and T. Saito, Hydromagnetic waves driven by velocity shear instability in the magnetospheric boundary layer, *Planet. Space Sci.*, *28*, 789, 1980.

Zhu, X., and M. G. Kivelson, Analytic formulation and quantitative solutions of the coupled ULF wave problem, *J. Geophys. Res.*, *93*, 8602, 1988.

Ziesolleck, C. W. S., and D. R. McDiarmid, Auroral latitude Pc5 field line resonances: Quantized frequencies, spatial characteristics, and diurnal variation, *J. Geophys. Res.*, *99*, 5817, 1994.

S. D. Bale, Space Sciences Laboratory, University of California, Berkeley, CA. (e-mail: bale@ssl.berkeley.edu)

G. Chisham, Astronomy Unit, Queen Mary and Westfield College, Mile End Road, London, E1 4NS, U.K. (e-mail: G.Chisham@qmw.ac.uk)

I. R. Mann, Department of Physics, University of Alberta, Edmonton, Alberta, Canada, T6G 2J1. (e-mail: imann@space.ualberta.ca)

(Received August 5, 1997; revised October 30, 1997; accepted October 31, 1997.)